THE UNIVERSITY OF RHODE ISLAND

University of Rhode Island
DigitalCommons@URI

Physics Faculty Publications

Physics

2013

pHLIP peptide targets nanogold particles to tumors

Lan Yao
University of Rhode Island

Jennifer Daniels
University of Rhode Island

See next page for additional authors

Follow this and additional works at: https://digitalcommons.uri.edu/phys_facpubs

Terms of Use
All rights reserved under copyright.

Citation/Publisher Attribution

Yao, L., Daniels, J., Moshnikova, A., Kuznetsov, S., Ahmed, A., Engelman, D. M., Reshetnyak, Y. K., & Andreev, O. A. (2013). pHLIP peptide targets nanogold particles to tumors. *Proc. Natl. Acad. Sci., 110*(2), 465-470. doi: 10.1073/pnas.1219665110 Available at: https://doi.org/10.1073/pnas.1219665110

This Article is brought to you for free and open access by the Physics at DigitalCommons@URI. It has been accepted for inclusion in Physics Faculty Publications by an authorized administrator of DigitalCommons@URI. For more information, please contact digitalcommons@etal.uri.edu.

Authors
Lan Yao, Jennifer Daniels, Anna Moshnikova, Sergey Kuznetsov, Aftab Ahmed, Donald M. Engelman, Yana Reshetnyak, and Oleg A. Andreev

This article is available at DigitalCommons@URI: https://digitalcommons.uri.edu/phys_facpubs/304

Corrections

APPLIED PHYSICAL SCIENCES, BIOPHYSICS AND COMPUTATIONAL BIOLOGY

Correction for "Cancer radiotherapy based on femtosecond IR laser-beam filamentation yielding ultra-high dose rates and zero entrance dose," by Ridthee Meesat, Hakim Belmouaddine, Jean-François Allard, Catherine Tanguay-Renaud, Rosalie Lemay, Tiberius Brastaviceanu, Luc Tremblay, Benoit Paquette, J. Richard Wagner, Jean-Paul Jay-Gerin, Martin Lepage, Michael A. Huels, and Daniel Houde, which appeared in issue 38, September 18, 2012, of *Proc Natl Acad Sci USA* (109:E2508–E2513; first published August 27, 2012; 10.1073/pnas.1116286109).

The authors note that they omitted a reference to an article by Dumont et al. The complete reference appears below.

Also, on page E2512, right column, third full paragraph, lines 1–3 "pGEM-3Zf(-) plasmid DNA (3,197 bp, Promega) was extracted form *Escherichia coli* DH5α and purified with the QIAfilter Plasmid Giga Kit (Qiagen)" should instead appear as "pGEM-3Zf(-) plasmid DNA (3,197 bp, Promega) was prepared in the laboratory of Dr. Darel Hunting. The plasmid was amplified and extracted from *Escherichia coli* JM109 and purified with the QIAfilter Plasmid Giga Kit (Qiagen) followed by removal of tris-EDTA buffer using homemade Sephadex G50 (Pharmacia) columns, according to the method published by Dumont et al. (56)."

Lastly, the following statement should be added to the Acknowledgments: "The authors wish to thank Dr. Darel Hunting for providing the plasmid DNA used in this work."

56. Dumont A, Zheng Y, Hunting D, Sanche L (2010) Protection by organic ions against DNA damage induced by low energy electrons. *J Chem Phys* 132(4):045102.

www.pnas.org/cgi/doi/10.1073/pnas.1301033110

ECOLOGY

Correction for "A common rule for decision making in animal collectives across species," by Sara Arganda, Alfonso Pérez-Escudero, and Gonzalo G. de Polavieja, which appeared in issue 50, December 11, 2012, of *Proc Natl Acad Sci USA* (109:20508–20513; first published November 28, 2012; 10.1073/pnas.1210664109).

The authors note that on page 20509, left column, first full paragraph, line 15, "$\alpha = (\log(a) + \log(1/0.95 - 1))/\log(s)$" should instead appear as "$\alpha = (\log(a) - \log(1/0.95 - 1))/\log(s)$". This typographical error does not affect the calculations or conclusions of the article.

www.pnas.org/cgi/doi/10.1073/pnas.1222108110

APPLIED BIOLOGICAL SCIENCES

Correction for "pHLIP peptide targets nanogold particles to tumors," by Lan Yao, Jennifer Danniels, Anna Moshnikova, Sergey Kuznetsov, Aftab Ahmed, Donald M. Engelman, Yana K. Reshetnyak, and Oleg A. Andreev, which appeared in issue 2, January 8, 2013, of *Proc Natl Acad Sci USA* (110:465–470; first published December 24, 2012; 10.1073/pnas.1219665110).

The authors note that the author name Jennifer Danniels should instead appear as Jennifer Daniels. The corrected author line appears below. The online version has been corrected.

Lan Yao, Jennifer Daniels, Anna Moshnikova, Sergey Kuznetsov, Aftab Ahmed, Donald M. Engelman, Yana K. Reshetnyak, and Oleg A. Andreev

www.pnas.org/cgi/doi/10.1073/pnas.1300604110

PHARMACOLOGY

Correction for "Local injection of dsRNA targeting calcitonin receptor-like receptor (CLR) ameliorates *Clostridium difficile* toxin A-induced ileitis," by Aditi Bhargava, Matthew S. Clifton, Pallavi Mhsake, Min Liao, Charalabos Pothoulakis, Susan E. Leeman, and Eileen F. Grady, which appeared in issue 2, January 8, 2013, of *Proc Natl Acad Sci USA* (110:731–736; first published December 24, 2012; 10.1073/pnas.1219733110).

The authors note that the author name Pallavi Mhsake should instead appear as Pallavi Mhaske. The corrected author line appears below. The online version has been corrected.

Aditi Bhargava, Matthew S. Clifton, Pallavi Mhaske, Min Liao, Charalabos Pothoulakis, Susan E. Leeman, and Eileen F. Grady

www.pnas.org/cgi/doi/10.1073/pnas.1301038110

pHLIP peptide targets nanogold particles to tumors

Lan Yao[a,1,2], Jennifer Daniels[a,2], Anna Moshnikova[a], Sergey Kuznetsov[a], Aftab Ahmed[b], Donald M. Engelman[c,3], Yana K. Reshetnyak[a], and Oleg A. Andreev[a,3]

[a]Physics Department, University of Rhode Island, Kingston, RI 02881; [b]Department of Biomedical and Pharmaceutical Sciences, College of Pharmacy, University of Rhode Island, Kingston, RI 02881; and [c]Department of Molecular Biophysics and Biochemistry, Yale University, New Haven, CT 06511

Contributed by Donald M. Engelman, November 12, 2012 (sent for review March 13, 2012)

Progress in nanomedicine depends on the development of nanomaterials and targeted delivery methods. In this work, we describe a method for the preferential targeting of gold nanoparticles to a tumor in a mouse model. The method is based on the use of the pH Low Insertion Peptide (pHLIP), which targets various imaging agents to acidic tumors. We compare tumor targeting by nonfunctionalized nanogold particles with nanogold–pHLIP conjugates, where nanogold is covalently attached to the N terminus of pHLIP. Our most important finding is that both intratumoral and i.v. administration demonstrated a significant enhancement of tumor uptake of gold nanoparticles conjugated with pHLIP. Statistically significant reduction of gold accumulation was observed in acidic tumors and kidney when pH-insensitive K-pHLIP was used as a vehicle, suggesting an important role of pH in the pHLIP-mediated targeting of gold nanoparticles. The pHLIP technology can substantially improve the delivery of gold nanoparticles to tumors by providing specificity of targeting, enhancing local concentration in tumors, and distributing nanoparticles throughout the entire tumor mass where they remain for an extended period (several days), which is beneficial for radiation oncology and imaging.

membranes | nanoparticle targeting | tumor acidity

Targeting of therapeutic nanoparticles could reduce side effects in treating cancer, as most antitumor drugs are toxic, killing not only tumor cells but also causing serious damage to healthy cells. One significant difference between tumors and normal tissues is that the former exhibit an acidic extracellular environment (1). Acidosis is a hallmark of tumor development both at very early and advanced stages (2, 3), as a consequence of anaerobic metabolism (the Pasteur effect) (4), the activity of carbonic anhydrases IX and XII (5), and the "aerobic glycolysis" known as the Warburg effect (6). Thus, the targeting of most solid tumors might be achieved by using pH-sensitive drugs and delivery systems.

We have been developing a unique approach for targeting acidic tissue, based on the family of pH (Low) Insertion Peptides (pHLIPs). pHLIPs are water-soluble, moderately hydrophobic polypeptides originally derived from the bacteriorhodopsin C helix. A pHLIP is triggered by acidity to fold and insert across a membrane to form a stable transmembrane alpha helix (7). At neutral pH, pHLIP is in equilibrium between soluble and membrane-bound unstructured forms, whereas in a low-pH environment, the protonation of negatively charged residues (Asp or Glu) (8, 9) enhances peptide hydrophobicity, increasing the affinity of the peptide for the lipid bilayer and triggering peptide folding and subsequent membrane insertion (8, 10). The Gibbs free energy of pHLIP binding to a 1-Palmitoyl-2-Oleoyl-sn-Glycero-3-Phosphocholine (POPC) from Avanti Polar Lipids liposome surface at 37 °C is about –7 kcal/mol near neutral pH, and the additional free energy of folding and insertion across a lipid bilayer at low pH is nearly –2 kcal/mol (11). Thus, the affinity of the peptide for a membrane at low pH is several times higher than at neutral pH, allowing pHLIP to distinguish and mark acidic diseased tissue (8, 10, 12, 13). We have shown that the N terminus of pHLIP stays outside of the bilayer, whereas the C terminus inserts across the lipid bilayer at low pH (14, 15). Small molecules (mostly imaging agents) covalently conjugated with the N terminus of pHLIP can be delivered to tumors where they are tethered to cell surfaces at low pH (12, 13, 16). As a control for pH targeting in vivo we have used K-pHLIP, where the Asp residues in the transmembrane part of a pHLIP are replaced by Lys residues. K-pHLIPs lack pH-dependent insertion into liposome phospholipid bilayers or cell membranes in vitro or in vivo (12, 13, 16). K-pHLIP labeled with fluorescent dyes and PET and Single-Photon Emission Computed Tomography (SPECT) agents show no targeting of tumors compared with the WT-pHLIP (12, 13, 16, 17). pHLIP peptides conjugated with optical and PET imaging probes are listed as pH targeting agents in the Molecular Imaging and Contrast Agent Database, National Center for Biotechnology Information. The results of a study demonstrating tumor targeting by SPECT-pHLIP has been published recently (17).

Davies et al. recently reported the pHLIP-mediated, pH-controlled delivery of 13 nm water-soluble gold nanoparticles coated with luminescent europium into human platelets in vitro (18). In related work presented here, we show that pHLIP not only induces the binding of 1.4 nm gold nanoparticles to cancer cells at acidic pH in vitro but also that it stabilizes binding in tumors established in mice. Gold is an inert and nontoxic material with unique properties suitable for many applications such as cancer diagnosis and treatment (19–21). For example, the irradiation of gold atoms at their k-edge excitation energy (soft X-rays) will generate Auger electrons or highly reactive species that may produce a clinically achievable dose enhancement of as much as 10-fold, capable of local inactivation of biological molecules (22, 23). The targeted delivery of gold to diseased tissue that we demonstrate here could lead to the successful application of gold nanoparticles in the diagnosis and treatment of tumors.

Results

Biophysical Studies. Changes of tryptophan fluorescence and CD spectral signals can be used to monitor pHLIP binding to a membrane lipid bilayer at neutral pH and insertion at lower pH (7). We found that nanogold attached to pHLIP significantly quenches tryptophan fluorescence, making it unreliable for use in monitoring pHLIP insertion into a membrane (nevertheless, a wavelength shift of the tryptophan fluorescence maximum was observed). Because gold nanoparticles are achiral in the UV range (24) and do not interfere with the CD signals of a peptide, we used the CD spectra of gold-pHLIP to study peptide–bilayer interactions. Our data show that pHLIP attached to nanogold is

Author contributions: Y.K.R. and O.A.A. designed research; L.Y., J.D., A.M., S.K., A.A., and O.A.A. performed research; L.Y., J.D., and O.A.A. analyzed data; and D.M.E., Y.K.R., and O.A.A. wrote the paper.

The authors declare no conflict of interest.

[1]Present address: Physics Department, Binghamton University, State University of New York, Binghamton, NY 13902.

[2]L.Y. and J.D. contributed equally to this work.

[3]To whom correspondence may be addressed. E-mail: andreev@mail.uri.edu or donald.engelman@yale.edu.

This article contains supporting information online at www.pnas.org/lookup/suppl/doi:10.1073/pnas.1219665110/-/DCSupplemental.

predominantly unstructured at pH 8.0 in the absence or presence of liposomes, whereas we observed helix formation at low pH in the presence of POPC liposomes (Fig. 1). Thus, we conclude that the attachment of gold nanoparticles to the N terminus of pHLIP did not interfere with the ability of the peptide to form a helical structure interacting with the membrane at low pH. Based on our other studies, we interpret these data to indicate that the pHLIP inserts into the membrane at low pH.

Nanogold Uptake by Cultured Cells. We compared the binding of gold-pHLIP or gold nanoparticles to cultured cells at neutral and low pHs. Nanoparticles (2 μM, 200 μL) were incubated with HeLa–GFP cells at pH 7.4 or 6.5. After 1 h, cells were washed, fixed, and stained with silver enhancement solution, resulting in the deposition of silver on gold nanoparticles to form micrometer-sized particles, which were visualized under a light microscope (Fig. 2). The images on Fig. 2 were analyzed according to Eq. **2** (*Methods*) to establish the ratios of gold (and silver) concentrations between the cells treated with gold-pHLIP or gold nanoparticles and the untreated cells at pH 7.4 and 6.5. Cells treated with gold-pHLIP nanoparticles at both pHs (Fig. 2 *C* and *G*) showed higher uptake of gold (threefold at pH 7.4 and 6.4-fold at pH 6.5) compared with cells treated with unmodified gold nanoparticles (Fig. 2 *B* and *F*). Cellular uptake of gold-pHLIP nanoparticles at pH 6.5 (Fig. 2 *G* and *H*) was 1.6 times higher than that at pH 7.4 (Fig. 2 *C* and *D*). These data demonstrated the pH-dependent, pHLIP-mediated uptake of gold nanoparticles by cells.

Animal Studies. When s.c. HeLa tumors reached 5–8 mm in diameter, they were intratumorally or i.v. injected with gold nanoparticles, gold-pHLIP, and gold-K-PHLIP conjugates. At 24 h after intratumoral administration of 15 μg gold or gold-pHLIP nanoparticles, mice were euthanized, and the tumors and major organs were harvested. The amount of gold in the tissues and organs was established by Inductively Coupled Plasma Mass Spectrometry (ICP-MS) analysis (Fig. 3*A* and Table S1). These results indicated that up to 8 μg (i.e., 54% i.d./g) of gold per gram of tumor was delivered by pHLIP and remained in the tumor after 24 h, compared to 0.7 μg/g (8% i.d./g) in the case of non-functionalized gold nanoparticles. Accumulation of gold was also observed in kidneys (about 2.1 μg/g). Because small particles

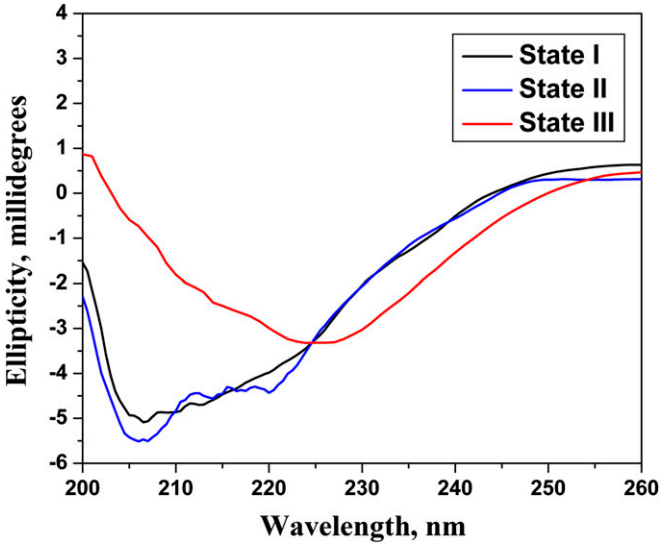

Fig. 1. CD spectra of gold-pHLIP in buffer pH 8.0 (state I) and in the presence of POPC liposomes at pH 8.0 (state II) and pH 4.0 (state III).

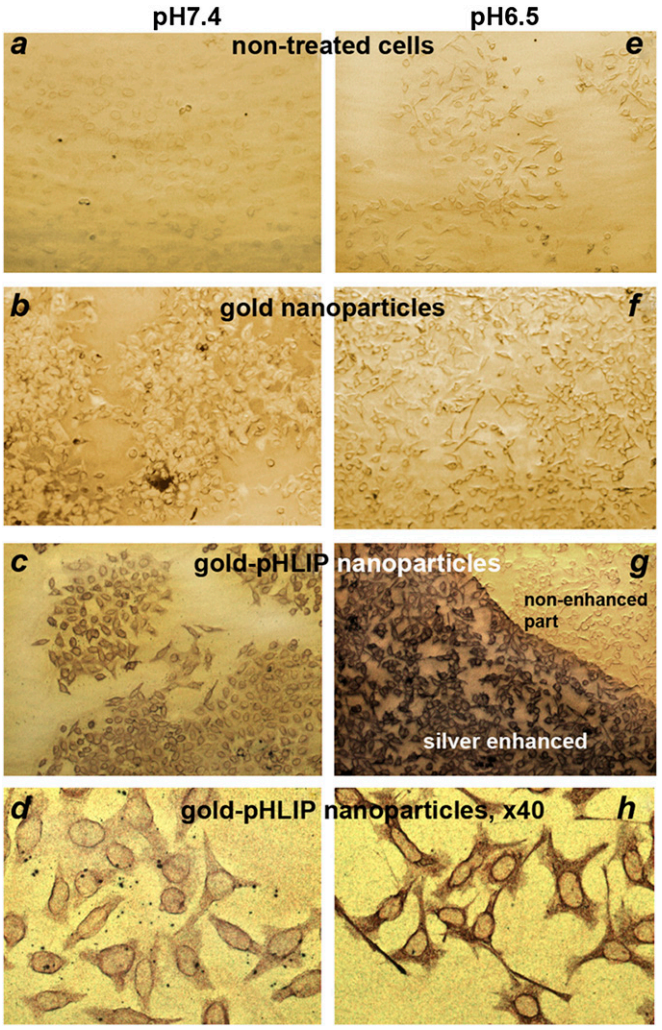

Fig. 2. Cellular uptake of gold-pHLIP and gold nanoparticles. Nanoparticles (2 μM, 200 μL) were incubated with HeLa-GFP cells at pH 7.4 or 6.5. After 1 h, cells were washed, fixed, and stained with silver enhancement solution, resulting in the deposition of silver on gold nanoparticles to form micrometer-sized particles, which were visualized under a light microscope The images *A–G* and *D–H* were taken with 10× and 40× objectives, respectively.

(1.4 nm) were used in this study, it is likely that clearance was predominantly urinary, as has been observed with fluorescent-, PET-, and SPECT-labeled pHLIP constructs (13, 17). We have previously observed that the pHLIP can accumulate in kidneys due to the low pH in the tubules (16, 25).

I.V. administration was given as two consecutive injections within 24 h. Split dosing was used to avoid high-concentration-mediated aggregation. Each injection contained 150 μL of 20 μM gold-pHLIP, gold-K-pHLIP, or nonfunctionalized gold particles (i.e., 45 μg). Necropsies were performed 24 h after the last injection. These data showed that 1.4 μg of gold per gram (1.5% i.d./g) of tissue was delivered by pHLIP to the tumors (Fig. 3*B* and Table S1). When pH-nonsensitive K-pHLIP was used as a delivery vehicle, tumor targeting was reduced threefold (0.47 μg/g or 0.5%). The uptake of gold-K-pHLIP was also reduced threefold in kidneys, and the distribution in other organs was similar to gold-pHLIP.

To assess distribution of these gold nanoparticles within the tissues, tumors, kidneys, and livers were collected and sectioned 4 h and 24 h after gold-pHLIP or gold nanoparticle administration. Silver enhancement was used to visualize the gold nanoparticles

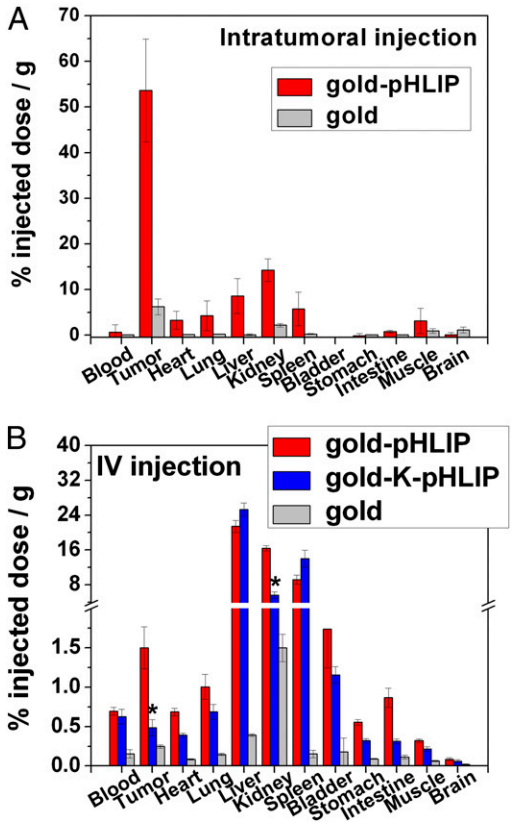

Fig. 3. ICP-MS analysis of the amount of gold in the excised tissues. Either a single intratumoral injection of gold-pHLIP or gold nanoparticles (*A*; 20 μM, 50 μL) or two i.v. injections of gold-pHLIP, gold-K-pHLIP, and gold (*B*; 20 μM, 150 μL each) were given to mice bearing s.c. tumors. Organs were collected at 24 h after the last injection. Organ uptakes of gold via intratumoral and IV injections are shown in *A* and *B*, respectively. The amount of gold per gram of tissue is given in Table S1. Mean ± SEM values are shown; $*P <$ 0.0001 vs. respective value of tumor uptake of gold targeted by gold-pHLIP.

in tissue sections. The same conditions of silver enhancement were used for all slides shown in Fig. 4. The amount of gold/silver correlated with the darkness of the tissue sections. These data show that gold distribution within the tumors, kidney, and liver were higher and uniform at both time points for gold-pHLIP injection than for unmodified gold administration.

The sections were further analyzed under a microscope with 10× (Fig. 5) and 100× (Fig. 6) objectives. The gold distribution in tumors and livers (Fig. 5 *D* and *L*) was homogeneous, in contrast to the distribution in kidneys (Fig. 5*H*), where the gold was mostly accumulated in the cortex. Cellular localization was confirmed by staining of cell nuclei with DAPI (Fig. 6). The images of the tumor sections demonstrated that pHLIP was distributed throughout the entire tumor mass, penetrating to the cells in the tumor interior and labeling the extracellular space and cellular membrane (Fig. 6 *A*–*C*).

Discussion

Gold nanoparticles are of interest as potential diagnostic and therapeutic agents in vivo, as they can be used as X-ray contrast agents (26), radiation enhancers (27), and laser (28, 29) and radiofrequency (30) thermotherapy enhancers. If tumors can be loaded with gold, this would lead to a higher dose to the cancerous tissue compared with the dose received by normal tissue during a radiotherapy treatment. Calculations indicate that the dose enhancement can be significant, as much as 200% or greater (27). Gold nanoparticles are not toxic: the LD_{50} of this material is ~3.2 g (Au) per kg of body weight^{-1} (26). Thus, the targeted delivery of gold nanoparticles could improve the treatment of cancers.

In general, one might suppose that specific delivery can be accomplished by conjugating gold or any other nanoparticle to antibodies or ligands that target proteins overexpressed on cancer cell surfaces, and this approach has been actively explored for many years for delivery of small molecules. However, several recent studies have raised serious questions on the efficacy of targeting ligands on nanoparticle accumulation in tumor tissues, showing that targeted nanoparticles did not accumulate more than nontargeted controls, although increased cellular uptake was observed in each case (31–33). In addition, histological studies revealed that gold nanoparticles conjugated with antibodies do not penetrate deeply into tumors, but mostly stain peripheral tumor regions (34). The direct injection of μm-sized gold particles does not lead to tumor targeting, as particles remain at the injection site and are not able to diffuse even within a tumor, hindering tumor coverage (22).

In the present work, we report the promising finding that pHLIP can enhance i.v. delivery of gold nanoparticles to tumors by sixfold. On the other hand, nano-sized gold particles with no conjugated pHLIP were washed out quickly from tumors and other organs. Targeting with the pH-insensitive K-pHLIP (wherein two Asp residues were replaced by Lys) resulted in statistically significant threefold reductions of gold accumulation. We interpret these data as showing that the preferential distribution of pHLIP-targeted gold is mediated by the acidosis present in tumors and kidneys. The direct injection of gold-pHLIP into tumors resulted in nearly uniform labeling of cancer cells with gold nanoparticles throughout the entire tumor, revealing that the pHLIP targeting allows migration within acidic regions to target the entire mass. Direct injection resulted in accumulation

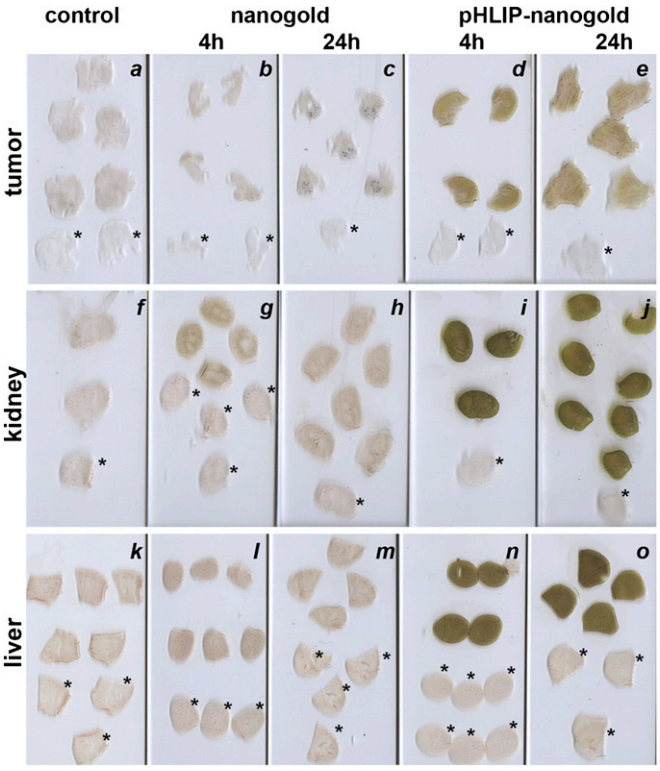

Fig. 4. Accumulation of gold-pHLIP (*D*, *E*, *I*, *J*, *N*, *O*) and gold nanoparticles (*B*, *C*, *G*, *H*, *L*, *M*) in tumor (*A*, *B*, *C*, *D*, *E*), kidney (*F*, *G*, *H*, *I*, *J*) and liver (*K*, *L*, *M*, *N*, *O*). Control tissues were taken from untreated mouse (*A*, *F*, *K*). The slices indicated by an asterisk were not treated with silver enhancement solution.

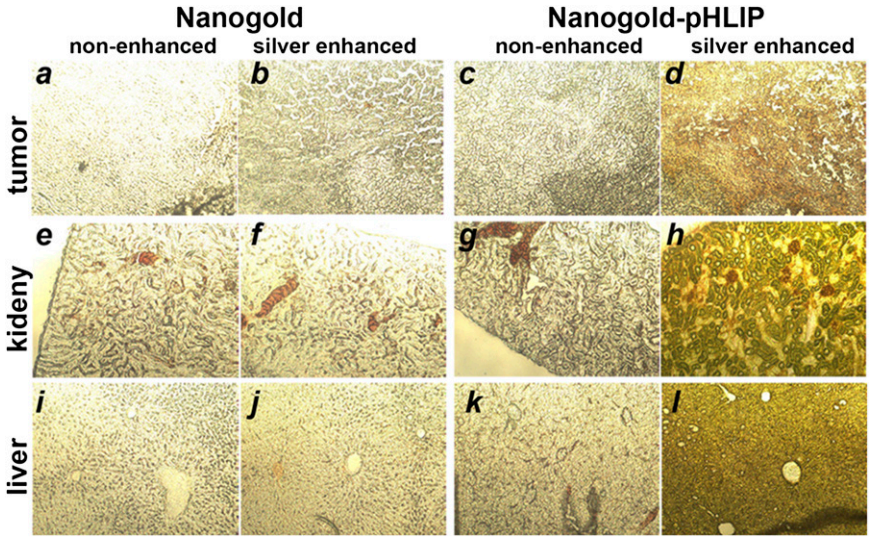

Fig. 5. Photomicrographs (10×) of tumor (*A*–*D*), kidney (*E*–*H*) and liver (*I*–*L*) sections non-enhanced (*A*, *E*, *I*, *C*, *G*, *K*) or enhanced (*B*, *F*, *J*, *D*, *H*, *L*) with silver after injection of nanogold (*A*, *B*, *E*, *F*, *I*, *J*) or nanogold-pHLIP (*C*, *D*, *G*, *H*, *K*, *L*) particles.

of 8.1 μg/g (54% i.d./g) in the tumor after 24 h. An *N*-fold increase in diameter gives N^3 increase in number of gold atoms per particle, so with gold particles of 14 nm it might be possible to increase the amount of gold 1,000-fold and to reach about 1% of gold of tumor mass, which is the amount that would be needed for a significant enhancement of the radiation therapeutic effect. Because the pHLIP-gold migrates to occupy the entire tumor, an excellent therapy might result.

This work demonstrates that pHLIP can mediate targeted delivery of nanoparticles to tumors and that direct injection can result in distribution throughout the tumor mass. Further improvements of nanoparticle coatings may be able to improve bioavailability, enhance tumor targeting, and reduce accumulation in nontarget organs. pHLIP technology can substantially improve the delivery of gold nanoparticles to primary tumors (and possibly metastatic lesions) by providing specificity of targeting, enhancing local concentrations, and improving retention in the tumor mass for an extended period (several days).

Methods

Peptide Conjugation with Gold Nanoparticles. The pHLIP (ACEQNPIYWARYADWLFTTPLLLLDLALLVDADET) and K-pHLIP (ACEQNPIYWARYAKWLFTTPLLLLKLALLVDADET) peptides were prepared by Dr. James I. Elliott at the W. M. Keck Foundation Biotechnology Resources Laboratory at Yale University. Monomaleimido Nanogold and nonfunctionalized particles (1.4 nm)

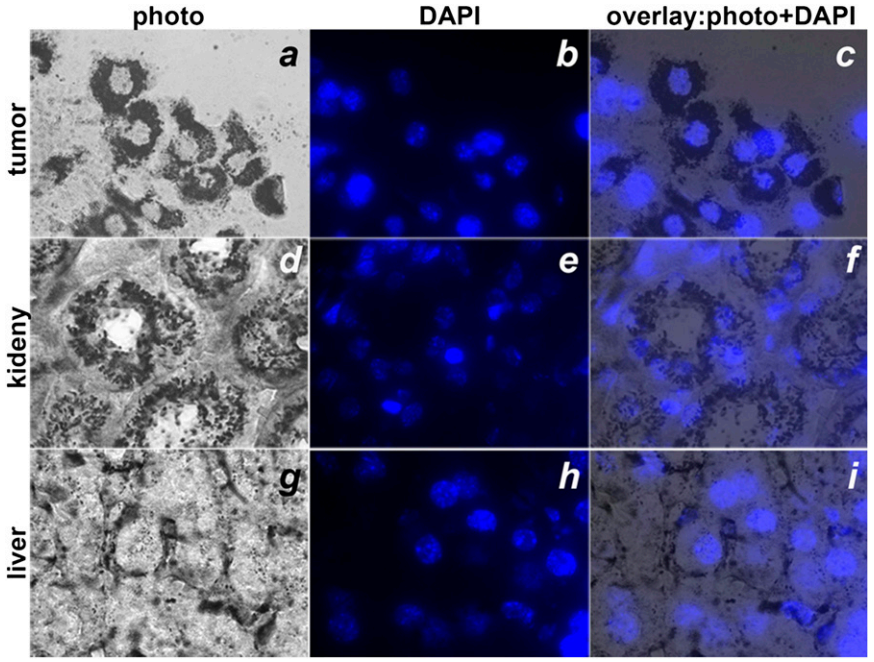

Fig. 6. Distributions of gold-pHLIP enhanced by silver in tumor (*A*, *B*, *C*), kidney (*D*, *E*, *F*) and liver (*G*, *H*, *I*). Slices were visualized under an inverted optical microscope with a 100× objective. The nuclei were stained with DAPI (blue color, *B*, *E*, *H*). Bright field (*A*, *D*, *G*) and fluorescent (*B*, *E* and *H*) images of the same sections and their overlays (*C*, *F*, and *I*) of tumor, kidney, and liver slices are presented.

were from Nanoprobes. A pHLIP peptide containing a single cysteine residue near its N terminus was conjugated with the single maleimide group on each nanogold particle. The progress of the coupling reaction was monitored by reversed phase HPLC. The concentration of peptide and nanogold was determined by absorbance at 280 nm (ε = 13,940 $M^{-1}{\cdot}cm^{-1}$) and 420 nm (ε = 155,000 $M^{-1}{\cdot}cm^{-1}$), respectively.

CD Measurements. CD measurements were carried out on a MOS-450 spectrometer (BioLogic) at 25 °C. Nonfunctionalized nanogold particles or nanogold-pHLIP conjugates were preincubated with 200 mol excess of POPC (1-Palmitoyl-2-Oleoyl-*sn*-Glycero-3-Phosphocholine from Avanti Polar Lipids) liposomes in 20 mM phosphate buffer, pH8.0. Liposomes with 50 nm diameter were prepared by extrusion. To induce the folding/insertion of peptide into the membrane lipid bilayer, HCl was added to lower the pH value from 8 to 4. CD signals of gold nanoparticles were taken as baseline signals and were subtracted from the corresponding signals of the nanogold-pHLIP conjugates.

Cell Lines. HeLa cells (human cervix adenocarcinoma, ATCC) without and with stable GFP expression were cultured in Dulbecco's Modified Eagle's Medium (DMEM) supplemented with 10% (vol/vol) FBS, 10 μg/mL of ciprofloxactin in a humidified atmosphere of 5% (vol/vol) CO_2 and 95% air (vol/vol) at 37 °C. Some cells were adapted by serial passages to improve growth in low pH medium (pH 6.5). The pH 6.5 medium was prepared by mixing 13.5 g of dry DMEM with 0.2 g of sodium bicarbonate in 1 L of deionized water.

Experiments on Cultured Cells. HeLa-GFP cells grown in pH 6.5 or 7.4 media were seeded in an eight-chamber slide (Lab-Tek, Thermo Scientific). At 80% confluency, cells were treated at pH 6.5 or 7.4 with 2 μM of nanogold or nanogold-pHLIP in 200 μL of serum-free DMEM at 37 °C under 5% CO_2. Cells not treated with nanogold were used as negative controls. After incubation for 1 h, the treatment solution was removed and cells were washed twice with serum-free DMEM (pH 7.4) and once with sterile PBS (pH 7.4). Subsequently, the cells were fixed with cold methanol at –20 °C for 15 min and then washed twice with sterile PBS (pH 7.4) and once with deionized water. After air drying, the chamber walls were removed and the cell slides were developed with freshly prepared HQ SILVER reagent (Nanoprobes). The reagent nucleates on the nanogold particles, resulting in the precipitation of metallic silver and the formation of micrometer-sized particles with low background. The developing time was varied until optimal conditions were found (about 20 min). Subsequently, the cell slides were rinsed twice with deionized water and viewed under a light microscope.

Estimation of Cellular Uptake of Gold/Silver Based on the Analysis of Cell Images. After silver staining, the brightfield images of cells were analyzed with the ImageJ program. For cells treated with nanogold, the mean intensities of the fields with cells (I_i) and without cells ($I_{0,i}$, background) were calculated. The concentration of gold/silver (c_i) can be represented as a mean intensity according to the Beer–Lambert law:

$$c_i = \frac{A_i}{\varepsilon d} = \frac{1}{\varepsilon d} ln \frac{I_{0,i}}{I_i}, \quad [1]$$

$$\frac{c_i}{c_{nt}} = \frac{ln\left(I_{0,i}/I_i\right)}{ln\left(I_{0,nt}/I_{nt}\right)}, \quad [2]$$

where A_i is the absorbance; ε is the extinction coefficient, and d is the thickness of the sample. For cells not treated with nanogold, c_{nt}, I_{nt}, and $I_{0,nt}$ correspond to the concentration of gold/silver, measured as the mean intensities of the fields with and without cells, respectively. We assume that the extinction coefficient and thickness are the same for all slides, so that the ratio of concentrations can be calculated according to Eq. **2** by knowing the mean intensities.

Tumor Targeting in Mice. Athymic female nude mice ranging in age from 4 to 6 wk and weighing from 15 to 18 g were obtained from Harlan Laboratories; 38 mice were used in the study. Mouse tumors were established by s.c. injection of HeLa cells (10^6 cells/0.1 mL/flank) in the right flank of each mouse. When tumors reached 5–8 mm in diameter, intratumoral or tail vein injections of nanogold samples were performed. For intratumoral injection, 50 μL of 20 μM nanogold or nanogold-pHLIP in sterile PBS (pH 7.4) was given at each of three different spots in each tumor. For tail vein injection, two consecutive injections of 150 μL of 20 μM nanogold-pHLIP or nonfunctionalized nanogold and nanogold-K-pHLIP as controls were given within 24 h. Animals were euthanized at 4 or 24 h after the last injection. Necropsy was performed immediately after euthanasia. Tumors and major organs were collected for further histological analysis and study using ICP-MS. Noninjected mice with similar-sized tumors were used as negative controls.

All animal studies were conducted according to the animal protocol AN07-01-015 approved by the Institutional Animal Care and Use Committee, University of Rhode Island, in compliance with the principles and procedures outlined in the National Institutes of Health Guide for the Care and Use of Animals.

Histological Analysis of Tumors and Organs. The excised tumors and organs were fixed in 4% formalin in PBS solution (pH 7.4) for 24 h at 4 °C. Tissues were then rinsed with sterile PBS (pH 7.4), blotted dry, and placed in 30% sucrose in PBS solution for at least 24 h at 4 °C. Samples were mounted in HistoPrep frozen tissue embedding medium (Fisher Scientific) and frozen in the quick freezer chamber of a cryostat (Vibratome UltraPro5000, GMI) at −80 °C. Samples were frozen only one time, to minimize tissue damage. When the temperature of mounted frozen samples was equilibrated with the working chamber temperature (−12 °C), the tissue was sectioned at a thickness of 10–20 μm. Sections were mounted on microscope slides coated with poly-lysine, dried in air, and washed with deionized water. Subsequently, silver enhancement of gold nanoparticles was carried out (developing time, 10 min). In some cases, further staining with DAPI was performed to stain cell nuclei. The stained section was covered with a drop of mounting medium (Permount, Fisher Scientific) and then a cover slide was placed over the medium. The slides were examined with an inverted fluorescence microscope (IX71 Olympus).

ICP-MS Analysis. Mouse tissue samples were dissolved in aqua regia, freshly prepared by mixing concentrated nitric and hydrochloric acids in a volume ratio of 1:3. If necessary, sonication or heating was used to facilitate the digestion of tissue samples. Then the concentrated sample solutions were diluted to 10 mL to give 2% nitric acid and analyzed via ICP-MS (ThermoScientific ×7 series) against calibration standards IMS 103 (UltraScientific).

ACKNOWLEDGMENTS. We thank Katherine Kelley for helping with ICP-MS, Bethany Healy-Rossi for the mouse injections, Sida Zheng and Renato Guerrieri for help in sample preparation for ICP-MS, and Ming An for reading the manuscript. We acknowledge financial support from the Department of Defense BC061356 (to O.A.A.) and National Institutes of Health (NIH) CA133890 (to O.A.A., D.M.E., and Y.K.R.). The Rhode Island IDeA Network of Biomedical Research Excellence core facility is funded by National Center for Research Resources/NIH P20RR016457.

1. Gatenby RA, Gillies RJ (2008) A microenvironmental model of carcinogenesis. *Nat Rev Cancer* 8(1):56–61.
2. Gillies RJ, Liu Z, Bhujwalla Z (1994) 31P-MRS measurements of extracellular pH of tumors using 3-aminopropylphosphonate. *Am J Physiol* 267(1 Pt 1):C195–C203.
3. Newell K, Franchi A, Pouysségur J, Tannock I (1993) Studies with glycolysis-deficient cells suggest that production of lactic acid is not the only cause of tumor acidity. *Proc Natl Acad Sci USA* 90(3):1127–1131.
4. Krebs HA (1972) The Pasteur effect and the relations between respiration and fermentation. *Essays Biochem* 8:1–34.
5. Swietach P, Hulikova A, Vaughan-Jones RD, Harris AL (2010) New insights into the physiological role of carbonic anhydrase IX in tumour pH regulation. *Oncogene* 29(50):6509–6521.
6. Warburg O, Wind F, Negelein E (1927) The metabolism of tumors in the body. *J Gen Physiol* 8(6):519–530.
7. Hunt JF, Rath P, Rothschild KJ, Engelman DM (1997) Spontaneous, pH-dependent membrane insertion of a transbilayer alpha-helix. *Biochemistry* 36(49):15177–15192.
8. Andreev OA, Engelman DM, Reshetnyak YK (2009) Targeting acidic diseased tissue: New technology based on use of the pH (Low) Insertion Peptide (pHLIP). *Chim Oggi* 27(2):34–37.
9. Musial-Siwek M, Karabadzhak A, Andreev OA, Reshetnyak YK, Engelman DM (2010) Tuning the insertion properties of pHLIP. *Biochim Biophys Acta* 1798(6):1041–1046.
10. Andreev OA, et al. (2010) pH (low) insertion peptide (pHLIP) inserts across a lipid bilayer as a helix and exits by a different path. *Proc Natl Acad Sci USA* 107(9):4081–4086.
11. Reshetnyak YK, Andreev OA, Segala M, Markin VS, Engelman DM (2008) Energetics of peptide (pHLIP) binding to and folding across a lipid bilayer membrane. *Proc Natl Acad Sci USA* 105(40):15340–15345.
12. Andreev OA, Engelman DM, Reshetnyak YK (2010) pH-sensitive membrane peptides (pHLIPs) as a novel class of delivery agents. *Mol Membr Biol* 27(7):341–352.
13. Vävere AL, et al. (2009) A novel technology for the imaging of acidic prostate tumors by positron emission tomography. *Cancer Res* 69(10):4510–4516.
14. Reshetnyak YK, Segala M, Andreev OA, Engelman DM (2007) A monomeric membrane peptide that lives in three worlds: In solution, attached to, and inserted across lipid bilayers. *Biophys J* 93(7):2363–2372.

15. Reshetnyak YK, Andreev OA, Lehnert U, Engelman DM (2006) Translocation of molecules into cells by pH-dependent insertion of a transmembrane helix. *Proc Natl Acad Sci USA* 103(17):6460–6465.
16. Reshetnyak YK, et al. (2011) Measuring tumor aggressiveness and targeting metastatic lesions with fluorescent pHLIP. *Mol Imaging Biol* 13(6):1146–1156.
17. Macholl S, et al. (2012) In vivo pH imaging with 99mTc-pHLIP. *Mol Imaging Biol* 14(6): 725–734.
18. Davies A, Lewis DJ, Watson SP, Thomas SG, Pikramenou Z (2012) pH-controlled delivery of luminescent europium coated nanoparticles into platelets. *Proc Natl Acad Sci USA* 109(6):1862–1867.
19. Huang X, Jain PK, El-Sayed IH, El-Sayed MA (2007) Gold nanoparticles: Interesting optical properties and recent applications in cancer diagnostics and therapy. *Nanomedicine (Lond)* 2(5):681–693.
20. Jain PK, El-Sayed MA (2007) Universal scaling of plasmon coupling in metal nanostructures: Extension from particle pairs to nanoshells. *Nano Lett* 7(9):2854–2858.
21. von Maltzahn G, et al. (2009) Computationally guided photothermal tumor therapy using long-circulating gold nanorod antennas. *Cancer Res* 69(9):3892–3900.
22. Herold DM, Das IJ, Stobbe CC, Iyer RV, Chapman JD (2000) Gold microspheres: A selective technique for producing biologically effective dose enhancement. *Int J Radiat Biol* 76(10):1357–1364.
23. Hainfeld JF, Slatkin DN, Smilowitz HM (2004) The use of gold nanoparticles to enhance radiotherapy in mice. *Phys Med Biol* 49(18):N309–N315.
24. Slocik JM, Govorov AO, Naik RR (2011) Plasmonic circular dichroism of Peptide-functionalized gold nanoparticles. *Nano Lett* 11(2):701–705.
25. Andreev OA, et al. (2007) Mechanism and uses of a membrane peptide that targets tumors and other acidic tissues in vivo. *Proc Natl Acad Sci USA* 104(19):7893–7898.
26. Hainfeld JF, Slatkin DN, Focella TM, Smilowitz HM (2006) Gold nanoparticles: A new X-ray contrast agent. *Br J Radiol* 79(939):248–253.
27. Hainfeld JF, Dilmanian FA, Slatkin DN, Smilowitz HM (2008) Radiotherapy enhancement with gold nanoparticles. *J Pharm Pharmacol* 60(8):977–985.
28. Mahmoud MA, El-Sayed MA (2010) Gold nanoframes: Very high surface plasmon fields and excellent near-infrared sensors. *J Am Chem Soc* 132(36):12704–12710.
29. Black KC, et al. (2008) Gold nanorods targeted to delta opioid receptor: Plasmon-resonant contrast and photothermal agents. *Mol Imaging* 7(1):50–57.
30. Glazer ES, et al. (2010) Noninvasive radiofrequency field destruction of pancreatic adenocarcinoma xenografts treated with targeted gold nanoparticles. *Clin Cancer Res* 16(23):5712–5721.
31. Sonvico F, et al. (2005) Folate-conjugated iron oxide nanoparticles for solid tumor targeting as potential specific magnetic hyperthermia mediators: Synthesis, physicochemical characterization, and in vitro experiments. *Bioconjug Chem* 16(5): 1181–1188.
32. Kirpotin DB, et al. (2006) Antibody targeting of long-circulating lipidic nanoparticles does not increase tumor localization but does increase internalization in animal models. *Cancer Res* 66(13):6732–6740.
33. Huang X, et al. (2010) A reexamination of active and passive tumor targeting by using rod-shaped gold nanocrystals and covalently conjugated peptide ligands. *ACS Nano* 4(10):5887–5896.
34. Haifeld JF, et al. (2011) Micro-CT enables microlocalisation and quantification of Her2-targeted gold nanoparticles within tumour regions. *Br J Radiol* 84(1002):526–533.